

# ASSESSMENT OF STRUCTURES REPEATEDLY EXPOSED TO THERMAL LOADING AND EXTINGUISHING WATER: A CASE STUDY OF A FIREFIGHTING TRAINING FACILITY

PETR MÜLLER, MARTIN BENÝŠEK, RADEK ŠTEFAN\*, JAKUB HOLAN,  
ŠÁRKA KOŠTÁLOVÁ

*Czech Technical University in Prague, Faculty of Civil Engineering, Department of Concrete and Masonry Structures, Thákurova 7, 166 29 Prague 6, Czech Republic*

\* corresponding author: [radek.stefan@fsv.cvut.cz](mailto:radek.stefan@fsv.cvut.cz)

**ABSTRACT.** When designing a new structure or assessing an existing one, the risk of fire and its effect on the structure must be considered. Structures are usually assessed for fire resistance at the design stage – i.e. before the possible exposure to fire. If structure is exposed to fire during its service life, a post-fire assessment must be conducted in order to evaluate whether the structure is still safe and reliable for use. The post-fire assessment is conducted quite regularly; however, the assessment is usually conducted for structures exposed to fire only once. This paper presents an interesting and unique case study of a post-fire structural analysis of a firefighting training facility exposed to cyclic fire loading and the effect of extinguishing water. The main conclusion of the study is that though means of protection are recommended, the structure still has a sufficient load-bearing capacity and can continue being used as a firefighting training facility in the future. Aside from the specific conclusions for the investigated structure, this paper presents the best practices and methods for the post-fire assessment of structures exposed to repeated fire loading, and can thus be used as a guidance by other engineers and researchers interested in this topic.

**KEYWORDS:** Fire, structural assessment, structural diagnostics, firefighting training facility, model of fire, CFD model, FDS software.

## 1. INTRODUCTION

Structures are usually assessed for fire resistance at the design stage – before possible occurrence of a fire. In case of a structure being exposed to fire, a post-fire assessment is required in order to evaluate whether the structure is still safe and reliable.

The main goal of a post-fire assessment is to determine the extent of structural damage. The extent of the damage depends on the specific thermal action, fire size, duration of the fire, ventilation conditions on one hand, and the actual fire resistance of the subjected structure on the other hand.

Some specific buildings are specially designed for repeated controlled fires. These buildings usually serve for firefighters as training facilities. The facilities serve for training of movement and orientation in a smoky space, exposure of firefighters to high temperatures, and possibly for training of the evacuation of inhabitants. One of these facilities is analysed in the present paper. The paper is based on an Expert Report [1] conducted by the authors.

The present paper focuses on a case study of a post-fire structural assessment of a training facility for firefighters. The assessment was conducted in order to evaluate the extent of the possible negative effects the fire trainings had on the structure in order to ensure the object's safe operation in the future.

The structural assessment of the whole building was

demanding by inner policy of the Czech Fire Rescue Service to specify the extent of the structural damage caused by repeating fire trainings.

As the building was originally not designed for this purpose, but has been used in this way for more than 10 years, the following questions must be answered:

- To what extent do fire trainings damage the structure?
- Is the structure reliable and safe enough to continue serving in the same manner in a long-term view?
- Is it necessary to repair the structure or to strengthen it?

The assessment of the analysed building consists of three tasks – (i) modelling of fire, (ii) structural diagnostics, and (iii) numerical assessment of the residual load-bearing capacity of the structure.

The first task – modelling of fire – is performed in order to simulate real fire scenario and evaluate the temperature evolution in the building. The Computational Fluid Dynamics (CFD) model of fire, implemented in the Fire Dynamics Simulator (FDS) [2], is employed for this analysis. The simulations help to determine the suitable positions of the steel and concrete specimens extracted from the structure, which are used for the laboratory testing of material properties and the subsequent assessment of the residual load-bearing capacity of the structure.

The second task consists of structural diagnostics. At first, a visual inspection is conducted. Based on the findings of the visual inspection of the building and the results of the fire modelling, the most fire-exposed parts of the load-bearing structure are identified. At these places, in-situ non-destructive testing of concrete is performed, and both concrete and steel specimens are extracted from the structure and tested in a laboratory in order to obtain actual residual material properties. The results of the material tests are compared to theoretical material deterioration models with respect to the temperatures obtained using the FDS simulations.

In the third task, a numerical assessment of the residual load-bearing capacity of the structure is conducted. Using the evolution of gas temperatures during fire obtained by the earlier fire-modelling, temperature distributions in the structure during fire are calculated. From the temperature distributions, theoretical material strength degradation according to Eurocode standards is calculated and compared with the results obtained by the in-situ and laboratory tests. The residual load-bearing capacity of the most fire-degraded structural elements is calculated and assessed and, further, appropriate refurbishments are designed.

The paper is organised as follows. The analysed building is described in Section 2. In Section 3, the model of fire is introduced. Section 4 deals with the structural diagnostics. The numerical assessment of the residual load-bearing capacity of the structure is performed in Section 5. In Section 6, all obtained results are presented and discussed. In Section 7, summarising conclusions are given.

## 2. DESCRIPTION OF THE ANALYSED BUILDING

The analysed building, see Figure 1, is being used as a training facility for firefighter trainees to experience fire-fighting before fighting real-scale fires. For such purposes, several gas burners producing flames, smoke, and high temperatures are installed inside the building. Although very high temperatures are reached during the trainings (up to  $1100^{\circ}\text{C}$  – according to the thermal power of each burner), the trainings last no more than 3 minutes. The main purpose of the trainings is to simulate conditions similar to those in real fire, which enables the trainees to practice movement and orientation in a smoky space, exposure to high temperatures, evacuation of occupants, or fire fighting. The fire fighting is performed by extinguishing water or other extinguishing media. The structure is thus not only affected by repeating thermal exposure due to the cyclic fire loading but also by the effect of the extinguishing media.

Within the preliminary inspection of the building, the construction system together with protection sub-structures were studied. Potential critical places were identified according to the positions of gas burners and



FIGURE 1. The analysed building.

visible deterioration of the structure. Also, detailed information needed for conducting the fire simulations was obtained by consulting with the building technicians. As a result of the preliminary inspection, the extent of forthcoming modelling of fire, structural diagnostics, and numerical assessment of the residual load-bearing capacity of the structure was determined.

The building has two above ground floors and one underground floor. Overall dimensions of the building are  $13\text{ m} \times 8\text{ m}$ , the height above the ground is  $7.5\text{ m}$ . The structural system consists of reinforced-concrete (RC) walls and slabs combined with steel floor beams. The RC walls are  $250\text{ mm}$  and  $200\text{ mm}$  thick. The RC slab above the underground floor is  $200\text{ mm}$  thick. The steel floor system above the first floor consists of I-shaped profile beams (IPE180) and steel decking. The roof system consists of steel beams and steel decking.

Structural members in rooms with gas burners are protected with soffit made of steel sheets. The gap between the structural members and the steel sheets is force-ventilated. The gap is force-ventillated not only during the fire trainings, but also a certain time before the training starts and after the training is finished. Thus, these structural members are not exposed to the flames, high temperatures, and fire-extinguishing water directly. During the structural diagnostics, the protective layers were removed to allow for both visual inspection and material sample extraction.

The fire training is demonstrated in Figures 2 and 3. The burners have a specific set-up, as they are partially covered by metal sheets to cluster and direct the flames, hot air, and smoke flow as shown in Figure 3. The gas burners are placed on the first and the second floors. On the underground floor, no burner is installed and hence, this floor is not analysed in detail in this paper. Five burners are installed in total. During a single fire training, only one burner is always active. The locations of the burners are shown in Figure 4.

## 3. MODELLING OF FIRE

Fire can be idealised by a model of fire. The basic mathematical models of fire are the nominal temperature-time curves (e.g. the standard



FIGURE 2. Initiation of a gas burner during the training.



FIGURE 3. A gas burner partially covered by metal sheets.

temperature-time curve ISO-834) which belong to the most conservative models. Models of fire which take the specific parameters related to the surrounding conditions and the fire itself as inputs are the natural fire models. These models can be simple – such as the local fire model and the parametric temperature-time curve (see [3]) – or advanced, which usually divide the space to a higher number of calculated zones or cells – such as zone models and Computational Fluid Dynamics models (CFD). These models are described in detail, e.g. in [3–14].

The last mentioned model, the CFD model, represents a modern approach with the ability to describe very specific fire scenarios assuming real conditions in the analysed space. Results of such calculations can be used for post-fire structural diagnostics and assessment – e.g. to get the probable temperature evolution in the analysed space and implement it for boundary conditions when analysing a structure and its behaviour during and after the fire, see [14–18].

The fire simulations discussed in this paper were conducted by NIST's FDS software [2]. As a pre-processor, the Pyrosim software [19] was used. For visualisation of results, the Smokeview software [20] was used. The model of the building is shown in Figure 5.

As only one gas burner is active during a fire training, four different simulations were performed, see

Figure 4. The fifth simulation with the gas burner on the left side of the second floor was not conducted since it was assumed that the results of such a simulation would be similar to the fourth simulation as the gas burners have the same thermal power and similar (corner) position. As an output of the fire simulations, temperature evolutions were obtained using the gas temperature thermocouples implemented in the model. The thermocouples are placed in the vicinity of potentially most affected structural members in a grid of  $0.5\text{ m} \times 0.5\text{ m}$ , see Figure 6.

Before conducting the fire simulations, detailed information about the fire trainings was gathered. Information needed for conducting the FDS simulations was obtained from building drawings and by consulting with building technicians. It also included the specification of burners thermal power and their shape, the position, and type of the used gas. The conditions in the analysed building during the trainings and the appropriate input data employed for the FDS simulations are summarised below:

- Only one burner is active during a fire training.
- Doors and gates are assumed as fully opened (both indoors and outdoors).
- Windows covered with metal sheet (highlighted by dashed lines with  $\times$  markers in the building layouts, see Figure 4), are omitted in the model.
- The protective layers (steel sheet soffit) are also included in the model according to their real position during the fire trainings. The force-ventilation of the gap between the load-bearing structures and the protective layer is neglected in the model.
- Burners are equipped with shielding plates which direct the flow of the hot gasses, as shown in Figure 3, and these plates are also simulated in the model.
- Material properties of surrounding structures are assumed as temperature-independent and taken from EN 1992-1-2 [21].
- The cell size in the model is set to  $0.2\text{ m} \times 0.2\text{ m} \times 0.2\text{ m}$  and the division method is set to uniform.
- Fire simulation time is 10 minutes in order to include the temperature evolution after the fire training is finished (3 minutes).
- The area of each burner is  $0.2\text{ m} \times 0.2\text{ m}$ . Each burner starts in  $t = 0.1\text{ s}$  with maximum released energy. Four simulations were conducted, each varying the position and the power of the burner. The power of the burner is either 1.5 MW or 3.0 MW, see Figure 4.

As a result, the fire simulations provide the overall evolutions of temperature distribution within the analysed building. These temperature evolutions were further utilised for the identification of the most fire-exposed parts of the load-bearing structure, where the

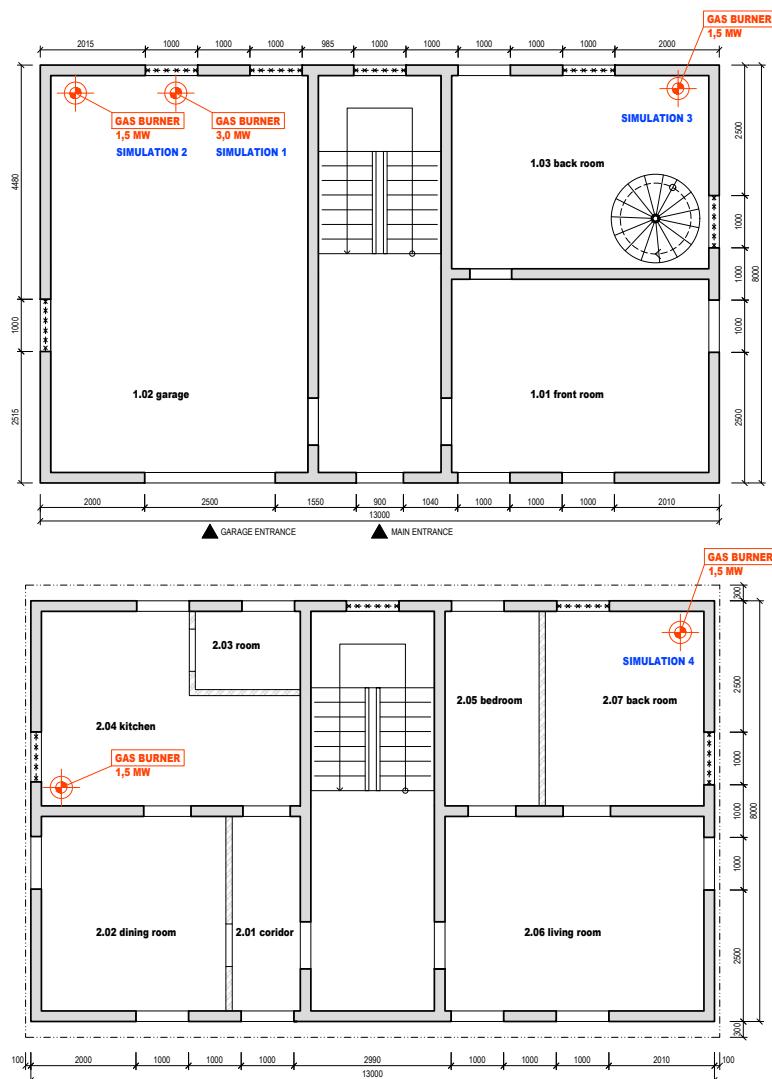


FIGURE 4. The locations and the power of the gas burners on the first floor (top) and on the second floor (bottom).

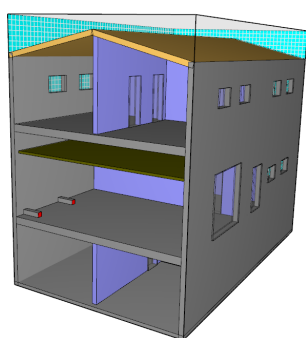


FIGURE 5. Overall visualization of the analysed building created using the Pyrosim software [19] (side wall is invisible).

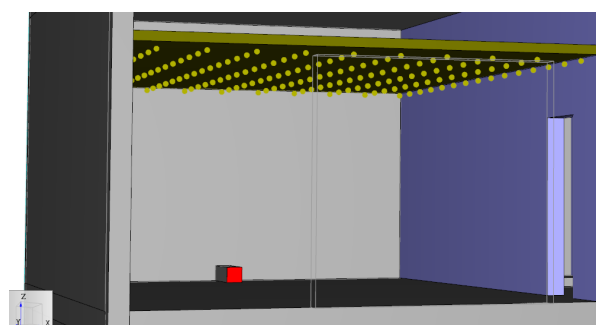


FIGURE 6. Visualisation of the thermocouples created using the Pyrosim software [19] (room 1.02; front wall is invisible).

structural diagnostic techniques were conducted – i.e. in-situ material tests and material samples extraction.

The results of the fire simulations were also used for the definition of boundary conditions in the detailed numerical thermal analysis of the analysed structural members – see further Sections.

## 4. STRUCTURAL DIAGNOSTICS

### 4.1. VISUAL INSPECTION

Based on the findings obtained during the preliminary inspection of the building and based on the results of the fire simulations, a detailed inspection of the building was carried out.

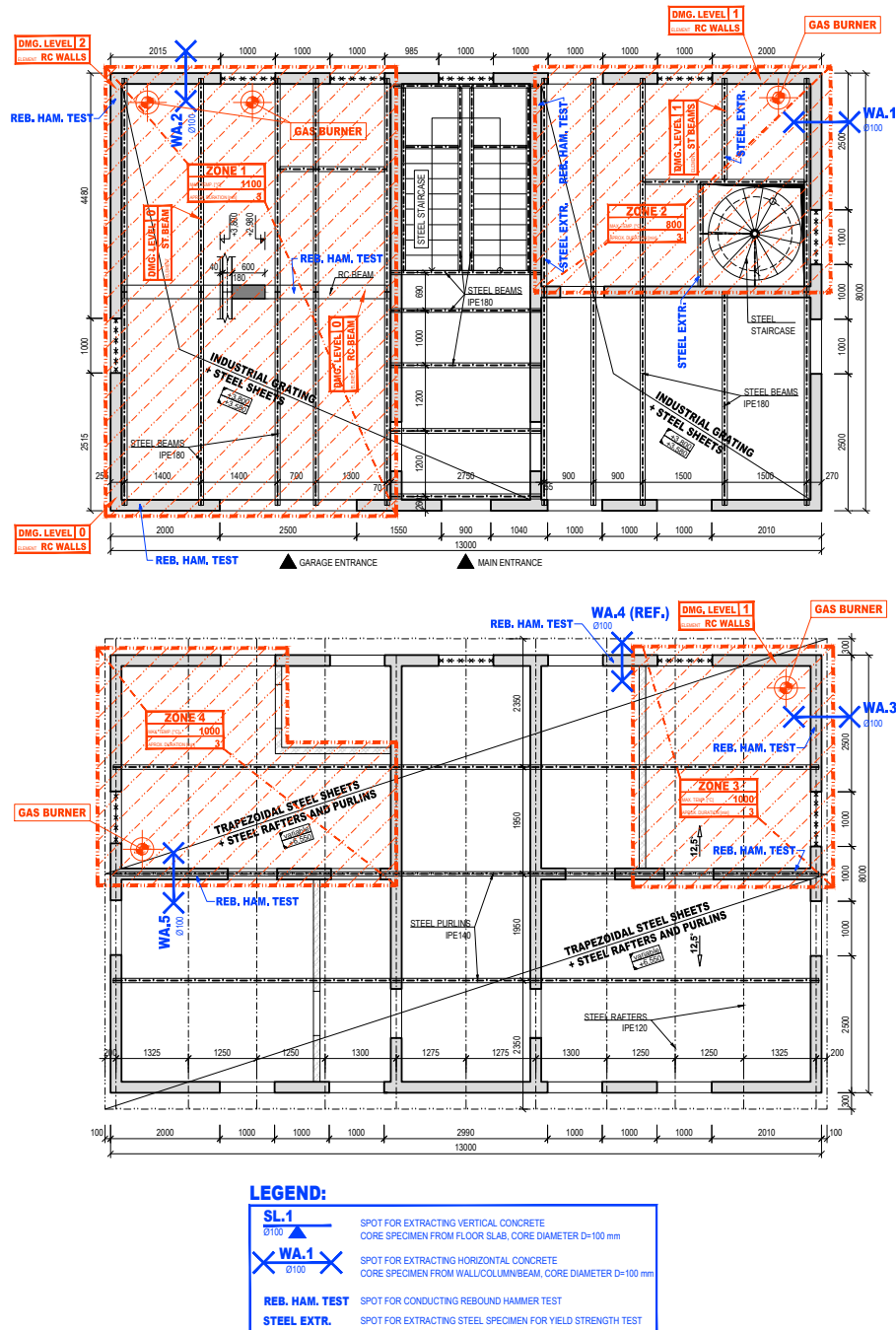


FIGURE 7. Layouts of the first floor (top) and the second floor (middle) with the information regarding the structural diagnostics; legend of the symbols used in the layouts (bottom).

All information regarding the structural diagnostics is summarised in building layouts, see Figure 7. Areas and structural members affected by the fire trainings were identified and drawn into the layouts. These areas were marked as ZONE 1 to ZONE 4. Maximum fire temperatures for each zone obtained by the aforementioned fire simulations as well as the duration of the fire are also given in the plans (for ZONE 4, the same temperature as for ZONE 3 was assumed). Individual structural elements were classified into damage classes according to their damage level determined by the visual inspection. The damage classification is done in accordance with the technical report pro-

posed by the Concrete society [22]. This technical report deals with the classification of concrete structures only, steel structures are not included. However, for the analysed building, the classification of steel elements was done analogically, i.e. Class 0 refers to *non-damaged element* while Class 4 refers to *totally damaged element*. The positions of the in-situ material tests and material samples extraction are given in the layouts as well.

On the basis of the visual inspection, it can be stated that RC structures do not exhibit significant damage nor extensive deflections. No places with a spalled cover layer were found, the reinforcement was



FIGURE 8. Flexural cracks with a width of 0.4–0.5 mm found on the bottom face of the RC slab above the underground floor (top) with observed leakage of fire-extinguishing water (bottom).

not exposed anywhere. Also, no buckled or ruptured rebars were found. Related to the fire trainings, sooted places on the structure were observed in the places where the hot airflow is directed to. Sooted places were also found in the vicinity of the opened windows, out of which the hot air leaves the building during the fire trainings. No surface crazing was found except for a few places above the windows. On the underground floor, flexural cracks with a width of 0.4–0.5 mm were found on the bottom face of an RC slab, see Figure 8. This defect causes a leak of the fire-extinguishing water when fire trainings are conducted on the floors above.

Steel structural elements of the floor/roof system above the first and second floors are in a very good condition since no evidence of corrosion, extensive deflections, buckling, nor distortion was found. This is probably due to the effective system of ventilated soffit. However, there is one exception – the soffit in the room with a spiral staircase in the first floor (ZONE 2) which was not ventilated. Therefore, some hot air may have accumulated in the space above the soffit, even though its majority flew to the second floor through the staircase opening due to the stack effect. Steel beams in this location are much more sooted and corroded, see Figure 9. However, no excessive deflections nor buckling were found. A detailed inspection of the beams in non-ventilated soffit revealed that the observed incoherent and sooted layers are a heat-damaged paint layer and fused pieces of soffit sheets.



FIGURE 9. Steel beams above the first floor near the spiral staircase, ZONE 2.

#### 4.2. IN-SITU NON-DESTRUCTIVE TESTING

To assess the surface deterioration of concrete (surface hardness reduction) in the space for fire trainings, a rebound hammer test was conducted, which is a method suitable for such purposes with only few limitations [23]. The results of a rebound hammer test usually assess the state of material degradation of an approximately 20–30 mm thick surface layer [24]. The rebound hammer test is illustrated in Figure 10. Rebound hammer tests were performed in selected places of the RC slab and walls on the underground floor and on the surfaces of beams and walls on the aboveground floors, see Figure 7.

Ten Q-value measurements for each testing place were carried out. The lowest and the highest measured values were excluded and the mean value and standard deviation were calculated from the remaining results. To convert the Q-values to the compressive strength, the standard conversion curve for modern concrete mixes proposed by the hammer manufacturer was used. The results were then adjusted according to the approach given in [25] based on the comparison with the laboratory destructive tests results.

#### 4.3. LABORATORY TESTING

Places for extracting concrete samples by core drilling were determined as described in the previous Sections, see Figure 7.

The diameter of the samples was 100 mm; the drill hole is visible in Figure 10 above the rebound hammer. The samples were tested in laboratory hydraulic press



FIGURE 10. Rebound hammer test.



FIGURE 11. Concrete core destructive compressive strength test.

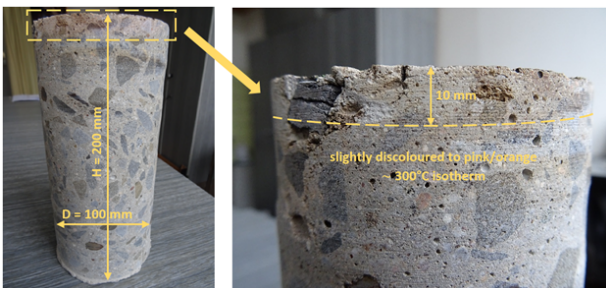


FIGURE 12. Concrete sample from ZONE 1 (WA.2) – estimation of approximate damage depth using colorimetry method.

to obtain concrete compressive strength, see Figure 11.

The samples obtained by core drilling consisted of a damaged concrete cover and an undamaged concrete core. During the compressive strength test, the whole specimen was tested. Thus, the obtained compressive strength is an average value representing the whole concrete sample including both its undamaged concrete core as well as its damaged concrete cover.

The depth of the damaged concrete cover was assessed using the colorimetry method, see [26]. Using this method, the depth of the damaged concrete cover was identified to be approximately 10 mm, see Figure 12.

Also, places for extracting steel samples out of steel elements in ZONE 2 were determined (4 samples from the bottom flange of I-beams and 4 pieces of supple-

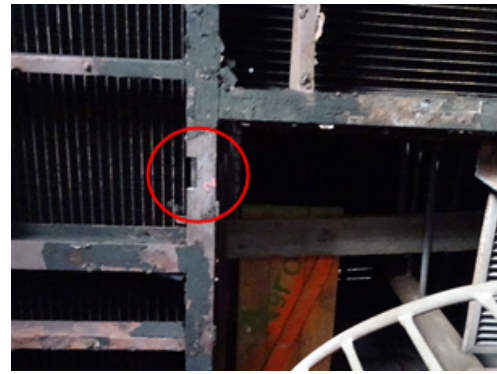


FIGURE 13. Steel sample cut out of floor beam in ZONE 2.



FIGURE 14. Steel yield strength test.

mentary soffit structure), see Figure 13.

The steel samples were then tested in laboratory by conducting the yield strength tests, see Figure 14.

## 5. NUMERICAL ASSESSMENT OF THE RESIDUAL LOAD-BEARING CAPACITY OF THE STRUCTURE

Based on the results of the visual inspection, fire simulations, and material tests, the assessment of the residual load-bearing capacity of the structure was carried out. In addition, the possibility of irreversible changes of the static scheme of the structural system was assessed. The results of the calculations were then used for the decision about the future usability of the building. Generally, three possible decisions could be made [26]: (i) the building is safe and reliable enough without any refurbishment, (ii) the structure has to be refurbished and/or strengthened (or acting loads reduced), or (iii) the building has to be demolished as the strengthening or refurbishment is either not possible or cost-effective.

Three types of structural elements were chosen for the detailed assessment.

- The residual load-bearing capacity was evaluated at the ultimate limit state (ULS) for the corner part of the outer load-bearing concrete wall near the gas burners in ZONE 1.

- The residual load-bearing capacity was evaluated at the ULS also for the steel floor beams in ZONE 2.
- For the RC slab above the underground floor, the assessment was performed at the ULS as well as at the serviceability limit state (SLS) since wide cracks were observed on this slab during the visual inspection.

### 5.1. THERMAL ANALYSIS OF SELECTED STRUCTURAL MEMBERS

Thermal analysis was conducted in order to determine the temperature distribution in the analysed structural elements. As a result of the fire simulations, the temperature-time curves were obtained. These temperature-time curves represent the gas temperature evolutions in the vicinity of the analysed RC wall and steel beam measured by the thermocouples in the FDS model. These temperature-time curves were then used for determining the heat flux assumed as the boundary condition within a heat transfer model. The heat flux was determined as a combined convective and radiative heat flux according to EN 1991-1-2 [3]. Detailed information about the heat transfer model used and its numerical solution can be found, e.g. in [27].

The thermal analysis of the RC wall was performed using an in-house software TempAnalysis [28]. The thermal analysis of the steel beam was performed using an incremental method in an in-house tool developed in MS EXCEL environment. Thermal properties describing concrete and steel behaviour at elevated temperatures were taken from EN 1992-1-2 [21] and EN 1993-1-2 [29].

Thermal analysis of the RC slab above the underground floor was not performed since the slab was not exposed to high temperatures on the bottom surface, and on the top – the heated surface, the slab was protected by 150 mm concrete flooring.

### 5.2. ASSESSMENT OF THE RESIDUAL LOAD-BEARING CAPACITY OF THE SELECTED STRUCTURAL MEMBERS

For the concrete wall in ZONE 1, the residual load-bearing capacity at ULS could be calculated using several different approaches, see e.g. [22, 30]. In this case, it was decided to lower the compressive strength of concrete for the whole cross-section according to results of concrete compressive strength tests, while the yield strength of the steel reinforcement was assumed the same as at a normal temperature. The load-bearing capacity was estimated using the N-M diagram.

In the case of the floor steel beams in ZONE 2, the assessment of the load-bearing capacity at ULS was conducted with initial material characteristics – as both the conducted tests of tensile strength of the samples and the conducted thermal analysis proved that the residual yield strength is not lower than the initial strength at a normal temperature.

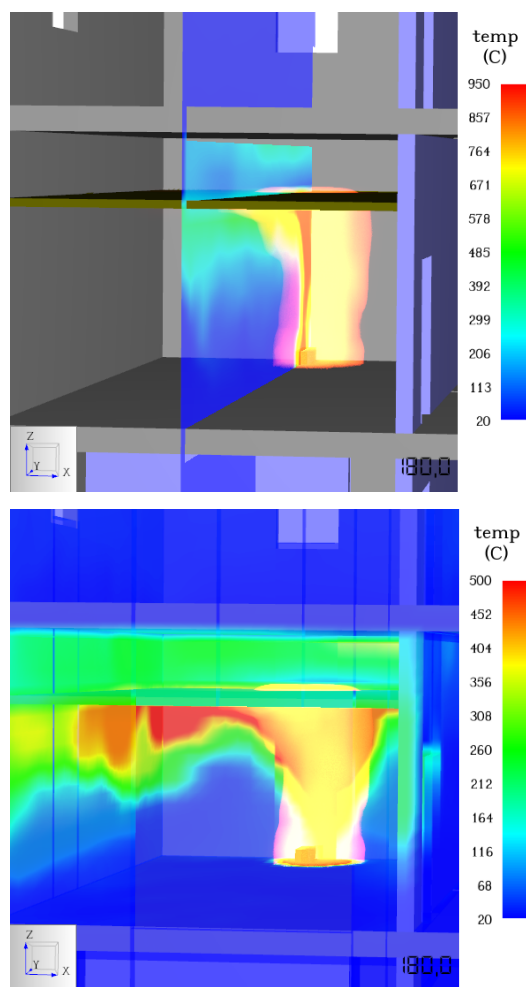


FIGURE 15. Simulation No. 1,  $t = 180$ s: gas temperatures (top); surface temperatures (bottom); front wall is invisible; visualised by the Pyrosim software [19].

The RC slab above the underground floor was assessed at ULS and SLS by assuming the initial material properties of concrete and steel reinforcement – i.e. the same as at normal temperature since the slab was not directly exposed to high temperatures (see above).

Since the post-fire situation is related to the ordinary ULS (and SLS) situation at a normal temperature, all loading and material safety factor values used in the calculation were assumed as for normal temperature calculations.

## 6. RESULTS AND DISCUSSION

Results from the three parts of the overall assessment of the analysed building (see Sections 3 to 5) are summarised and discussed in this Section. Conclusions derived from the results are then given in Section 7.

### 6.1. FIRE MODELLING RESULTS

Four different simulations were performed, see Section 3 and Figure 4.

The results from the first simulation (i.e. simulation No. 1) are shown in Figure 15. Moreover, in order to present a detailed description of the results, the

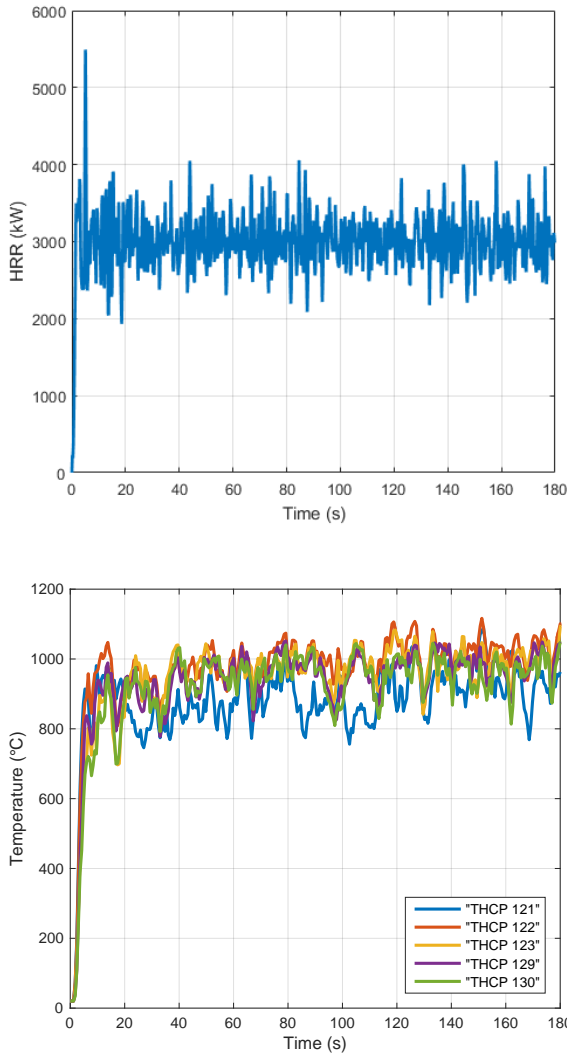


FIGURE 16. Simulation No. 1: heat release rate measured in FDS [2] (top); gas temperature evolution (in °C) measured by five thermocouples above the burner with the highest gas temperatures (bottom); visualised by the Pyrosim software [19] and the FMC software [31].

graphs of thermocouple temperatures and the heat release rate from the simulation No. 1 are shown in Figure 16. For a comparison, five thermocouples at various locations with the highest temperatures above the burner were chosen. In this simulation, a gas burner with the power of 3.0 MW was used, see Figures 4 and 16. As can be seen in Figure 16, the gas temperatures around the ceiling reached the maximum value of approximately 1 100 °C.

The results from the second simulation (i.e. simulation No. 2) are shown in Figure 17. In this simulation, a gas burner with the power of 1.5 MW was used, see Figure 4. In this simulation, the gas temperatures reached only approx. 800 °C, which is probably the result of the lower power (and lower value of the HRR) of the gas burner.

The results of simulation No. 3, with the burner

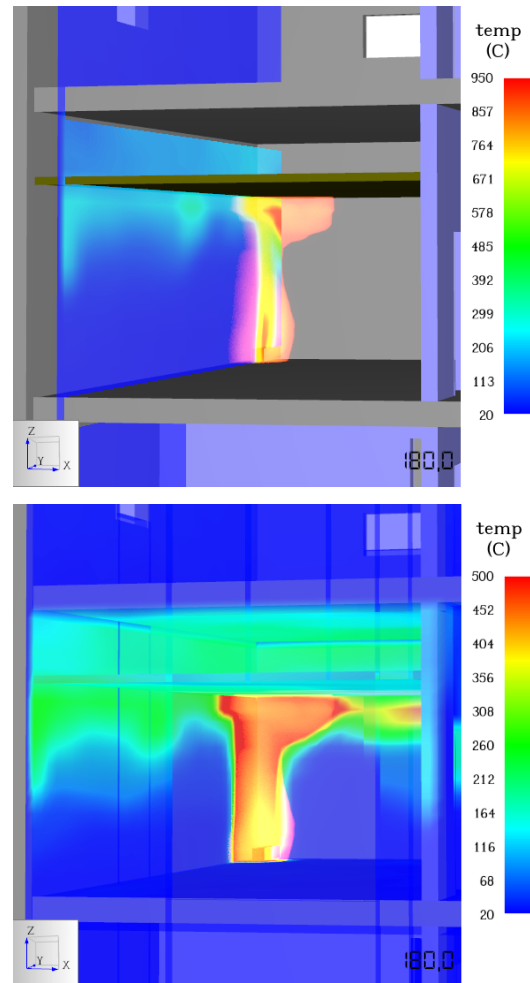


FIGURE 17. Simulation No. 2,  $t = 180$  s: gas temperatures (top); surface temperatures (bottom); front wall is invisible; visualised by the Pyrosim software [19].

set to 1.5 MW, are shown in Figure 18. It can be seen that the hot gases go through the spiral staircase into the room 2.07, where the uncovered steel structures are exposed to high temperatures. The shielding plates, which direct the flow of the hot gasses, are placed around the burner. Hence, the hot gasses flow back to the side wall. The space above the ceiling of the room No. 1.03 is not force-ventilated, thus the high temperatures affect the ceiling structures. In simulation No. 3, the gas temperatures around the ceiling reach the maximum value of approximately 800 °C.

The burner with HRR of 1.5 MW for simulation No. 4 is placed in room 2.07, see Figure 4. The results are shown in Figure 19. In this case, the maximum gas temperatures reach approximately 1 000 °C and the shielding plates direct the flow of the hot gasses.

## 6.2. STRUCTURAL DIAGNOSTICS RESULTS

The compressive strength of the concrete cover layer obtained by the rebound hammer test in the reference places (surfaces of unexposed structures) was ~ 38 MPa, which is closely similar to the results of

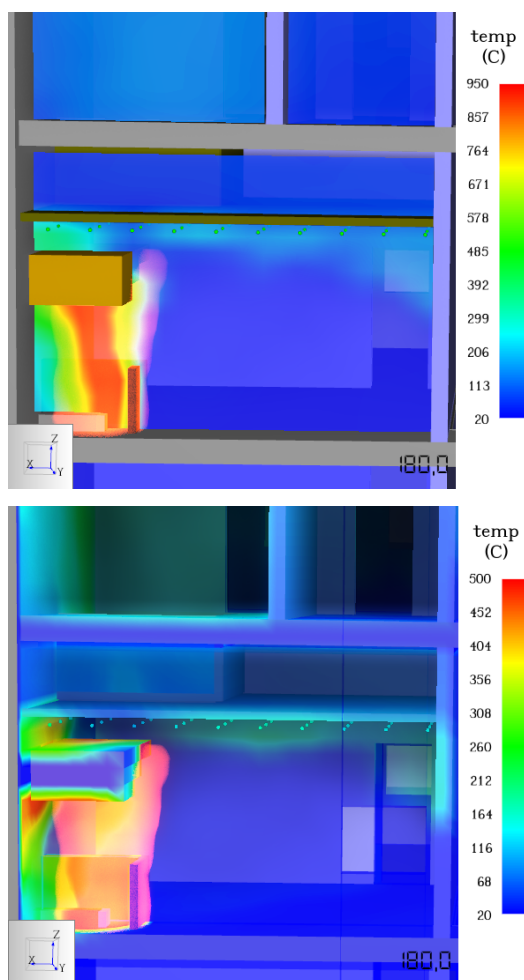


FIGURE 18. Simulation No. 3,  $t = 180$  s, gas temperatures (top); surface temperatures (bottom); back wall is invisible; visualised by the Pyrosim software [19].

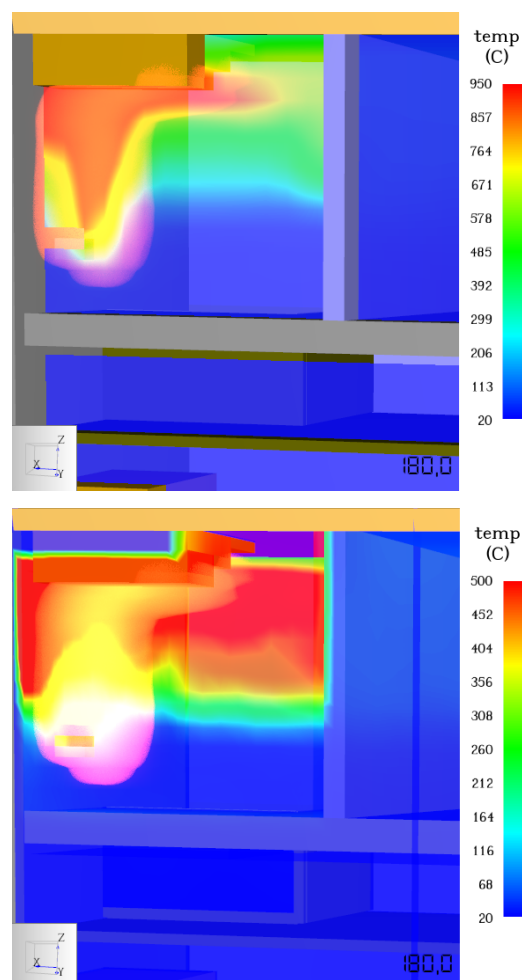


FIGURE 19. Simulation No. 4,  $t = 180$  s, gas temperatures (top); surface temperatures (bottom); back wall is invisible; visualised by the Pyrosim software [19].

reference destructive tests (see below). For ZONES 1–4, the results of the rebound hammer tests can be summarised as follows. Concrete cover compressive strength measured in the places farther from the burners or on the protected parts of the structure (beams and upper part of walls above soffit) are almost the same as the ones measured in the reference places. Concrete cover compressive strength measured in the vicinity of the burners is 20 % lower than the values measured in the reference places.

The results of the laboratory destructive test of concrete compressive strength are as follows. For the reference sample WA.4 (see Figure 7), compressive strength of  $f_{c,cyl} = 42.6$  MPa was measured. The compressive strength class of concrete in RC structures given in as-built documentation is C30/37 with mean compressive strength  $f_{cm} = 38$  MPa according to EN 1992-1-1 [32]. Compressive strength of sample WA.2 (ZONE 1, see Figure 7) was measured to be  $f_{c,is} = 31.9$  MPa (where the subscript “is” stands for “in structure”, see EN 13791 [33]). Compressive strength of sample WA.3 (ZONE 3, see Figure 7) was measured to be  $f_{c,is} = 41.1$  MPa. Compressive strength of sample WA.5 (ZONE 4, see Figure 7) was

measured to be  $f_{c,is} = 24.8$  MPa. This value corresponds with the concrete strength class C16/20 with the mean compressive strength  $f_{cm} = 24$  MPa according to EN 1992-1-1 [32]. The other samples exhibited unacceptable types of failure during the compressive strength test, and hence, the results were omitted from the analysis. The unacceptable type of failure means that in this case, some samples exhibited the shear failure mode or the side fractures at the ends. This was probably due to the fact that the top and bottom surfaces of the samples were not perfectly plain and also because the samples may have been damaged during the core drilling or during the subsequent manipulation.

As for steel components, the measured values of yield strength of steel samples cut out of the structure were in the range  $f_{y,is} = 284.9$ – $383.8$  MPa, which is above the limit value of the yield strength of the steel strength class S235. The class S235 is given in the as-built documentation, and therefore, no reduction of steel properties was expected. The measured values of strain at failure of the steel samples were in the range 16.2–33.5 %, which indicates a sufficient ductility of

steel.

### 6.3. RESULTS OF THE RESIDUAL

#### LOAD-BEARING CAPACITY ASSESSMENT

For determining the heat flux as a boundary condition for the thermal analysis of the RC wall in ZONE 1, mean values of the gas temperatures presented in Figure 16 were used, see Figure 20. The gas-temperature evolutions given in Figure 16 show the highest gas temperatures above the burner in ZONE 1. The gas temperatures were measured by the thermocouples in the FDS model. The “mean-values” curve given in Figure 20 adequately represents the whole range of these maximum temperatures and hence, employing this curve for determining the boundary condition for the analysed wall can be considered to be a conservative approach.

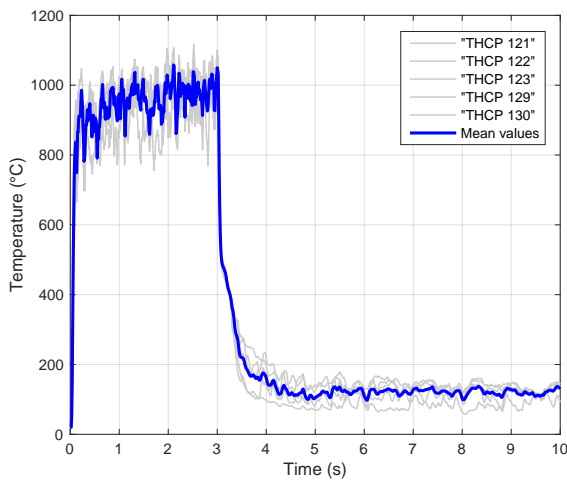


FIGURE 20. Temperature-time curve for ZONE 1 assumed for the heat transfer model boundary condition.

The results of the thermal analysis of the RC wall in ZONE 1, obtained using an in-house software TempAnalysis [28], are shown in Figure 21.

The results reveal that at the time when the fire training is terminated (i.e.  $t = 3$  min), the surface temperature of the RC wall reaches almost  $800^{\circ}\text{C}$ . This temperature causes a significant degradation of concrete; however, since the exposure time was short (i.e.  $t = 3$  min), only small part (few millimetres) of the concrete cover is heated up to this temperature and most of the inner concrete remains unheated. As can be seen in Figure 21, with increasing time, the maximal temperatures in concrete decrease rapidly.

The temperature distributions presented in Figure 21 show that only a 10 mm surface layer is heated to temperatures higher than  $300^{\circ}\text{C}$ . Based on this finding, it is expected that the reduction of mechanical properties takes place only in this surface layer. This presumption is validated by the aforementioned indicative colorimetry analysis which indicated that the

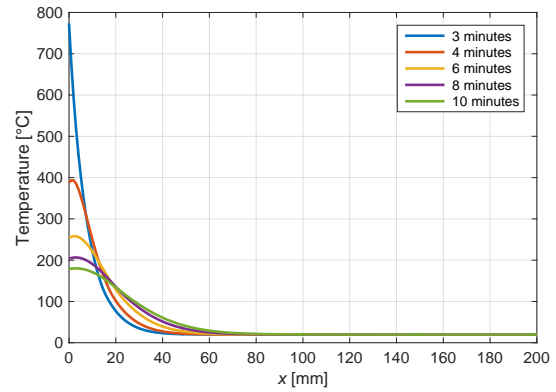


FIGURE 21. Temperature profiles of the analysed wall in ZONE 1.

depth of the damaged concrete is also approximately 10 mm – see the discoloured layer of the specimen in Figure 12.

According to EN 1992-1-2 standard [21], the theoretical reduction of compressive strength for the average temperature of the surface layer (i.e.  $250\text{--}300^{\circ}\text{C}$ ) is in the range of 15–20%. This value corresponds well with the experimentally obtained results, where the observed reduction of hardness and compressive strength was in the range of 17–20%.

From Figure 21, it is obvious that the steel reinforcement is protected by the concrete cover as at the distance of 20 mm from the heated surface, the temperature is lower than  $150^{\circ}\text{C}$ . Hence, it can be assumed that yield strength of steel reinforcement is the same as at a normal temperature.

Although it was proved that the degradation of mechanical properties of concrete takes place in the concrete cover only, it was decided to calculate the residual load-bearing capacity of the RC wall in ZONE 1 by assuming the compressive strength of concrete for the whole cross-section lowered according to the lowest strength measured by the laboratory destructive compressive strength test. This represents the most conservative approach ensuring indisputable safety of the obtained results.

The concrete compressive strength was lowered by three concrete strength classes (from C30/37 to C16/20). The load-bearing capacity was estimated using N-M diagram, see Figure 22. Since the post-fire situation is related to the ordinary ULS situation at a normal temperature, all loading and material safety factor values used in the calculation were assumed as for normal temperature calculations. The calculation reveals that the point representing loading lies inside the diagram with a sufficient reserve in load-bearing capacity, see Figure 22.

For determining the heat flux as a boundary condition for the thermal analysis of the steel beams in ZONE 2, maximum gas temperatures obtained by the fire simulations were used. The maximum gas temperatures were measured near the ceiling above

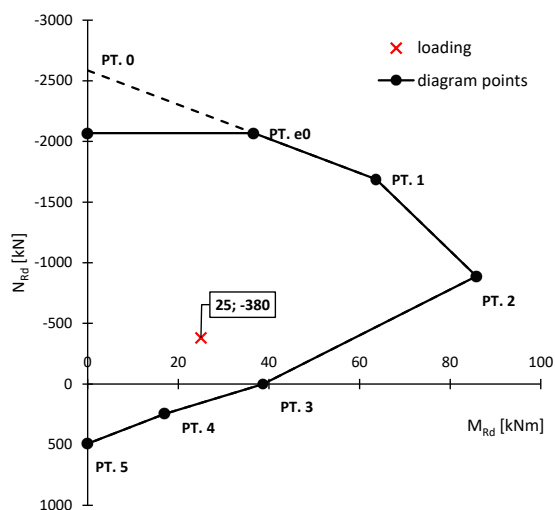


FIGURE 22. N-M diagram of load-bearing RC wall in ZONE 1 proving sufficient residual load-bearing capacity.

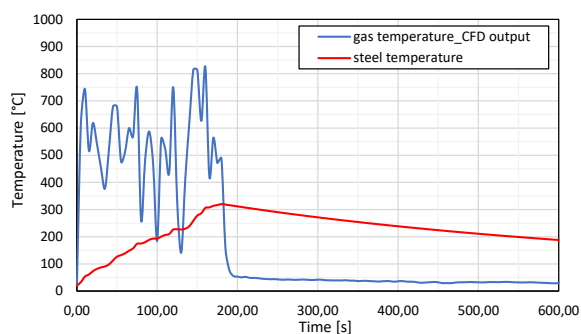


FIGURE 23. Comparison of gas temperatures of the space and surface temperature of the analysed steel beam in ZONE 2.

the burner in ZONE 2 in the FDS model. Not all of the fire-exposed steel beams are placed in the location above the burner, however, employing the maximum gas temperatures for determining the boundary condition can be considered to be a conservative approach.

The corresponding temperature-time curve is presented in Figure 23 together with the results of the thermal analysis of the beam performed using the incremental method.

The results reveal that the temperature of the steel beams located in ZONE 2 reached approximately 350 °C. This value does not reduce the yield strength, either in the hot or residual state (e.g. [34, 35]), and thus, the steel preserves its initial yield strength. The results of destructive material tests also confirmed that no significant reduction of yield strength took place. Although the temperature around 350 °C can slightly reduce other mechanical properties of steel (e.g. the elastic modulus or the proportional limit) in the hot state – see EN 1993-1-2 [29], these changes are supposed to be reversible and can be omitted in the residual state – see e.g. [34, 35]. Hence, the mechanical properties of steel are assumed to be not affected

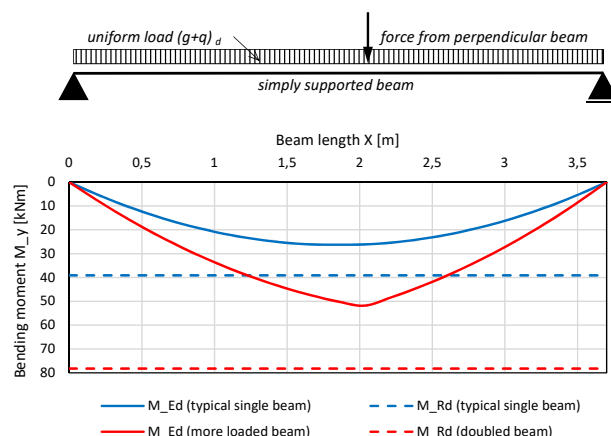


FIGURE 24. Diagram of bending moment along floor steel beam in ZONE 2.

by the high-temperature exposure for the assessment of the residual load-bearing capacity of the analysed steel beam.

In order to analyse the steel beam in ZONE 2, a diagram of bending moment along the beam length was calculated, and the load-bearing capacity was determined and depicted in the diagram, see Figure 24. Since the assessment refers to the state after the fire when the structure has to fulfil the same requirements as an undamaged structure, all loading and material safety factor values used in the calculation were assumed as for normal temperature calculations. The lateral torsional buckling of steel beams was not incorporated in the calculation due to the ensured stability of compressed upper flanges of beams by connected floor layers. Based on the diagram, it can be stated that the load-bearing capacity of a typical steel floor beam is sufficient. However, the longitudinal beam going along the opening for the staircase was additionally loaded by a transverse beam. The opening was made in the floor additionally and the structural consequences were not reflected. Thus, the bending moment of the mentioned beam exceeds the load-bearing capacity of a single beam. Since it was not possible to lower the acting loads (mainly live loads), it was proposed to double the beam with another IPE180 profile. The load-bearing capacity of such a doubled-beam is then sufficient, see Figure 24. Nevertheless, the designed strengthening is not related to fire trainings and their effect on the structure but to a previous unprofessional modification of the structure.

The RC slab above the underground floor was assessed at ULS and SLS by assuming the initial material properties of concrete and steel reinforcement since the slab was not directly exposed to high temperatures. The calculations proved that the slab satisfies both the ULS and SLS criteria. However, for the SLS – crack control, the calculated effective crack width is close to the limit crack width. This is in accordance with the findings of visual inspection (see Section 4.1 and Figure 8) whereby flexural cracks with

a width of 0.4–0.5 mm were found on the bottom face of the RC slab. This defect causes a leakage of the fire-extinguishing water when fire trainings are conducted on the floors above. From a long-term point of view, the presence of water and air near the reinforcement can cause its corrosion. A corrosion of reinforcement gradually lowers load-bearing capacity and durability of the structure. To resolve this problem, refurbishment measures were recommended – to improve the drainage system in the building and to repair waterproofing in floor layers.

## 7. CONCLUSIONS

Specific quantitative and qualitative results obtained through structural diagnostics and numerical assessment are presented in the Section above. In this last Section, overall conclusions are summarised and recommendations for refurbishment are provided.

Specific conclusions regarding the current state of the investigated structure after the repeated exposure to fire and extinguishing water are presented below.

- Since the structure was exposed to three-minute-long fires only, the reduction of mechanical properties of concrete occurred only in the concrete cover. It seems that the repeated exposure to fire has no significant cumulative effect on the structure that could affect the concrete core. This conclusion is supported by the numerical assessment as well as the destructive and non-destructive tests.
- Since the structure was exposed to three-minute-long fires only, the temperature of the steel beams did not reach values which would lower the yield strength of steel. It seems that the repeated exposure to fire has no significant cumulative effect on the mechanical properties of steel. This conclusion is also confirmed by the destructive yield strength tests.
- The laboratory destructive compressive strength test showed a reduced compressive strength of concrete. However, the obtained reduced strength is mainly induced by the degradation of the concrete cover and not the concrete core.
- Even when assuming the reduced strength of concrete for the whole cross-section when calculating the residual load-bearing capacity of the RC walls (which is a very conservative approach), a sufficient reserve in load-bearing capacity is obtained.
- Only one significant structural weakness was identified. However, the weakness and the proposed strengthening is not related to the fire exposure but to a previous unprofessional modification of the structure.

Specific proposed refurbishments for the investigated structure are presented below. It is recommended to:

- repair the concrete cover of the concrete structural members,

- repaint the steel structural members,
- repair the parts of the structural members where the material samples for destructive tests were extracted,
- improve the drainage system in the building and repair waterproofing in the floor layers (especially the ground floor),
- supplement the longitudinal beam going along the opening for the staircase with an additional IPE180 profile.

The main specific conclusion regarding the investigated structure is that the structure still has a sufficient load-bearing capacity, which was not significantly lowered by the fire trainings, and can continue being used as a firefighting training facility in the future. However, minor refurbishments are recommended in order to ensure long-term safety of the structure.

As this paper aims at being a guidance for other researchers interested in the topic of post-fire assessment of structures exposed to repeated fire and extinguishing water, general conclusions regarding these structures are presented below. If the structure is exposed to short-term fires only (up to 3 minutes) and the structural members are protected by steel soffits then:

- the reduction of mechanical properties of concrete occurs only in the concrete cover,
- the yield strength of steel is not affected,
- no significant cumulative effect of the repeated fire exposure on the material properties can be expected,
- the effect of the extinguishing media on the structure must be assessed, particularly when a significant crack width is observed in any concrete structural members.

The main general conclusion regarding structures exposed to repeated fire and extinguishing water is that for structures exposed to short-term fires only, with structural members protected by steel soffits, it is unlikely that significant damage will occur. However, it must be noted that when assessing these structures, consideration must be given not only to the fire exposure but also to the extinguishing-water exposure.

Aside from the specific conclusions for the investigated structure, this paper presents the best practices and methods for the post-fire assessment of structures exposed to repeated fire loading, and can thus be used as a guidance by other engineers and researchers interested in this topic. FDS simulations have proven to be a suitable complement to traditional structural diagnostics methods and post-fire assessment calculations.

The best practices and methods for the post-fire assessment of concrete structures are also summarised and analysed in detail in the doctoral thesis by the first author of this paper [36].

## ACKNOWLEDGEMENTS

This work has been supported by the Grant Agency of the Czech Technical University in Prague, projects SGS22/033/OHK1/1T/11 and SGS23/033/OHK1/1T/11. The support is gratefully acknowledged.

## REFERENCES

- [1] P. Müller, M. Benýšek, J. Procházka. Znalečný posudek nosných konstrukcí „ohňového domu“ [Expert Report on Assessment of Firefighting Training Facility], 2019.
- [2] K. McGrattan, S. Hostikka, R. McDermott, et al. Fire Dynamics Simulator User's Guide. NIST Special Publication 1019, Sixth Edition, 2018. <https://doi.org/10.6028/NIST.SP.1019>
- [3] EN 1991-1-2. Eurocode 1: Actions on structures – part 1-2: General actions – actions on structures exposed to fire, 2002.
- [4] A. H. Buchanan. *Structural Design for Fire Safety*. Wiley, 2002.
- [5] J. A. Purkiss. *Fire safety engineering, Design of structures*. Elsevier, 2nd edn., 2007.
- [6] G. H. Yeoh, K. K. Yuen. *Computational Fluid Dynamics in Fire Engineering*. Butterworth-Heinemann, Burlington, 2009.
- [7] M. Hurley, D. Gottuk, J. R. Hall Jr., et al. *SFPE handbook of fire protection engineering*. Springer, 5th edn., 2016. <https://doi.org/10.1007/978-1-4939-2565-0>
- [8] D. Drysdale. *An Introduction to Fire Dynamics*. Wiley, 3rd edn., 2011.
- [9] U. Wickström. *Temperature Calculation in Fire Safety Engineering*. Springer, 2016. <https://doi.org/10.1007/978-1-4939-2565-0>
- [10] J. Zehfuss, D. Hossier. A parametric natural fire model for the structural fire design of multi-storey buildings. *Fire Safety Journal* **42**(2):115–126, 2007. <https://doi.org/10.1016/j.firesaf.2006.08.004>
- [11] H. Xue, J. C. Ho, Y. M. Cheng. Comparison of different combustion models in enclosure fire simulation. *Fire Safety Journal* **36**(1):37–54, 2001. [https://doi.org/10.1016/S0379-7112\(00\)00043-6](https://doi.org/10.1016/S0379-7112(00)00043-6)
- [12] X. Dai, S. Welch, O. Vassart, et al. An extended travelling fire method framework for performance-based structural design. *Fire and Materials* **44**(3):437–457, 2020. <https://doi.org/10.1002/fam.2810>
- [13] J. E. Floyd, K. B. McGrattan, S. Hostikka, H. R. Baum. CFD fire simulation using mixture fraction combustion and finite volume radiative heat transfer. *Journal of Fire Protection Engineering* **13**(1):11–36, 2003. <https://doi.org/10.1177/1042391503013001002>
- [14] M. Benýšek. *Analysis of Fire Resistance of Concrete Structures Based on Different Fire Models*. Ph.D. thesis, CTU in Prague, 2021.
- [15] D. Kolaitis, E. Asimakopoulou, M. Founti. CFD Simulation of Fire Spreading in a Residential Building: The Effect of Implementing Phase Changing Materials. In *European Combustion Meeting*, pp. 1–6. 2011.
- [16] F. Wald, I. Burgess, G. Rein, et al. *COST TU0904: Integrated Fire Engineering and Response – Case Studies*. COST and CTU in Prague, 2012.
- [17] F. Pesavento, M. Pachera, P. Brunello, B. A. Schrefler. Concrete exposed to fire: From fire scenario to structural response **711**:556–563, 2016. <https://doi.org/10.4028/www.scientific.net/KEM.711.556>
- [18] C. Zhang, J. G. Silva, C. Weinschenk, et al. Simulation methodology for coupled fire-structure analysis: modeling localized fire tests on a steel column. *Fire Technology* **52**:239–262, 2016. <https://doi.org/10.1007/s10694-015-0495-9>
- [19] PyroSim User Manual. Thunderhead Engineering, 2018.
- [20] G. P. Forney. Smokeview, A Tool for Visualizing Fire Dynamics Simulation Data, Volume I: User's Guide. NIST Special Publication 1017-1, Sixth Edition, 2018.
- [21] EN 1992-1-2. Eurocode 2: Design of concrete structures – part 1-2: General rules – structural fire design, 2004.
- [22] Technical Report No. 68 – Assessment, design and repair of fire-damaged concrete structures. The Concrete Society, 2008.
- [23] P. Müller, J. Novák, J. Holan. Destructive and non-destructive experimental investigation of polypropylene fibre reinforced concrete subjected to high temperature. *Journal of Building Engineering* **26**:100906, 2019. <https://doi.org/10.1016/j.jobe.2019.100906>
- [24] P. Panedpojaman, D. Tonnayopas. Rebound hammer test to estimate compressive strength of heat exposed concrete. *Construction and Building Materials* **172**:387–395, 2018. <https://doi.org/10.1016/j.conbuildmat.2018.03.179>
- [25] ČSN 73 2011. Non-destructive testing of concrete structures, 2012.
- [26] *fib. Bulletin 46. Fire design of concrete structures – structural behaviour and assessment*. fib, 2008.
- [27] R. Štefan. *Transport Processes in Concrete at High Temperatures. Mathematical Modelling and Engineering Applications with Focus on Concrete Spalling*. Ph.D. thesis, CTU in Prague, 2015.
- [28] R. Štefan, J. Procházka. TempAnalysis - Computer program for temperature analysis of cross-sections exposed to fire. CTU in Prague., 2009.
- [29] EN 1993-1-2. Eurocode 3: Design of steel structures – part 1-2: General rules – structural fire design, 2005.
- [30] *fib. Bulletin 38. Fire design of concrete structures – materials, structures and modelling*. fib, 2007.
- [31] M. Benýšek, R. Štefan. FMC – Fire Models Calculator. CTU in Prague, 2015–2018.
- [32] EN 1992-1-1. Eurocode 2: Design of concrete structures – part 1-1: General rules and rules for buildings, 2004.
- [33] EN 13791. Assessment of in-situ compressive strength in structures and precast concrete components, 2020.
- [34] C. Maraveas, Z. Fasoulakis. Post-fire mechanical properties of structural steel. In *8th National Steel Structures Conference*, pp. 1–8. 2014.

[35] C. Maraveas, Z. Fasoulakis, K. D. Tsavdaridis. Post-fire assessment and reinstatement of steel structures. *Journal of Structural Fire Engineering* **8**(2):181–201, 2017. <https://doi.org/10.1108/JSFE-03-2017-0028>

[36] P. Müller. *Analysis of Concrete Structures after Fire*. Ph.D. thesis, CTU in Prague, 2022. .